Noname manuscript No.
(will be inserted by the editor)

UBCx Phot1x Design Proposal

Tony Cao

the date of receipt and acceptance should be inserted later

Abstract A simple beginner's project on seeing the impact of varying the waveguide width or waveguide length difference of a Mach-Zehnder Interferometer.

1 Introduction

edX username: tony_cao_

Mach-Zehnder Interferometers (MZI) are a widely used component in silicon photonics. One key characteristic that can be modified in a MZI is the path difference . The path difference of a MZI is the difference between the lengths of the waveguides in each arm, and changes the free spectral range of the MZI. In this project, I will be varying the path difference of a simple Mach-Zehnder Interferometer in order to see the impact it has on the free spectral range and group index. For each path difference, I will be fabricating two devices to test manufacturing variablity.

2 Theory

For the project I used a simple Mach-Zehnder Interferometer design with 2 TE polarized 1550nm fiber grating couplers, two Y-branch 50/50 splitters, and two strip waveguides. Since the I am using 50/50 splitters, the light in each arm should be equal. Thus, the intensity is given by:

$$I_1 = \ I_2 = \frac{I_{inital}}{2}$$

And the electric field is given by:

$$E_1 \ = \ \frac{E_{intial}}{\sqrt{2}}, \ E_2 \ = \ \frac{iE_{intial}}{\sqrt{2}}$$

Tony Cao
Affiliation not available

For the balanced interferometer I am using, the output of the Y-branch splitter is given by:

$$E_o = \frac{E_i}{2}\left(e^{-i\beta_1 L_1 - \frac{\alpha_1}{2}L_1} + e^{-i\beta_2 L_2 - \frac{\alpha_2}{2}L_2}\right)$$

And the intensity is given by:

$$I_o = \frac{I_i}{4}\left|e^{-i\beta_1 L_1 - \frac{\alpha_1}{2}L_1} + e^{-i\beta_2 L_2 - \frac{\alpha_2}{2}L_2}\right|^2$$

Since I will be studying the Free Spectral Range (FSR) of the different path differences, I will use:

$$FSR = \frac{\lambda^2}{n_g \cdot \Delta L},\ n_g = \frac{\lambda^2}{FSR \cdot \Delta L}$$

3 Modelling and Simulation

I will be using strip waveguides that are 500nm wide and 220nm tall, as well as TE polarized. The TE mode profile of the waveguide was generated by LUMMERICAL MODE and is given depicted below.

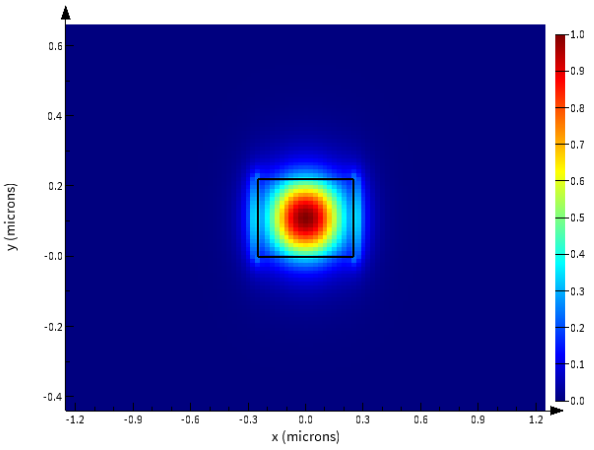

Fig. 1 TE Mode of Waveguide

The effective and group index were simulated against wavelength, from 1500nm to 1600nm.

Using MATLAB, the compact model of the waveguide is the following:

$$n_{eff}(\lambda) = 2.445 - 1.134(\lambda - \lambda_0) - 0.063(\lambda - \lambda_0)^2$$

MATLAB's graph of the effective index is depicted below.

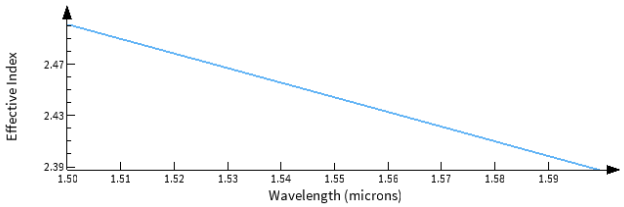

Fig. 2 Effective Index of Waveguide

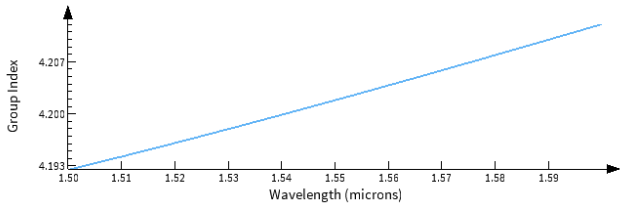

Fig. 3 Group Index of Waveguide

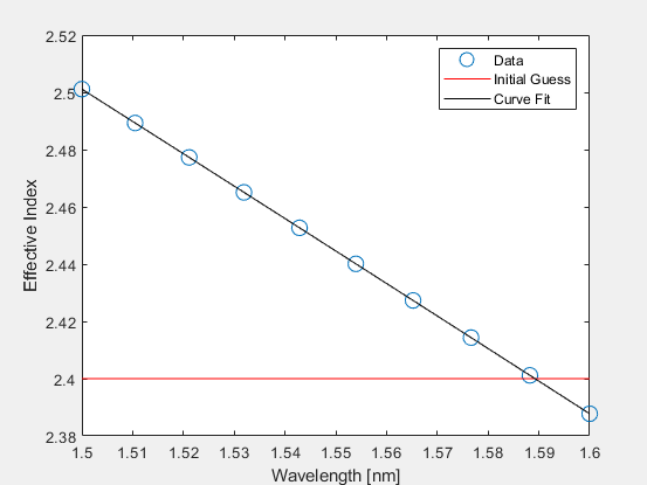

Fig. 4 Effective Index of Waveguide from MATLAB

From the theory part of this proposal, we know the transfer function of the unbalanced interferometer. If we assume that we are in a lossless medium, the transfer function becomes:

$$T(\lambda) = \frac{1}{2}\left[1 + \cos\left(\beta \Delta L\right)\right]$$

I will be testing out 5 different path differences, 50 micron, 100 micron, 150 micron, 200 micron, and 250 micron. The original waveguide length will be 10

micron. We can analytically calculate the FSR at 1550nm with a group index of 4.2 from *Fig 3* using equation (5).

ΔL(μm)	FSR(nm)
50	11.44
100	5.72
150	3.81
200	2.86
250	2.29

Table 1 Path Difference versus FSR

Using LUMERICAL INTERCONNECT, the Mach Zehnder Interferometers were simulated. The transmission spectra for a path difference of 50 micron, 150 micron, and 250 micron are below. Path differences of 100 micron and 200 micron are absent for the sake of visual clarity. Red depicts a path difference of 50 micron, green is 150 micron, and blue is 250 micron.

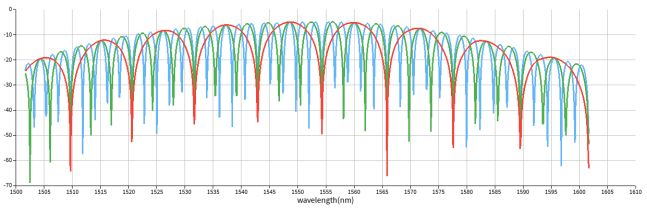

Fig. 5 Spectra of 50, 150, & 250 micron Path Difference

4 Fabrication

Due to fabrication difficulties, the waveguide may not always be the desired dimension of 220nm thick and 500nm wide. In order to better understand the variability in device performance that may arise from these challenges, corner analysis was performed on the 220nm thick and 500nm wide waveguide. The four corners that were analyzed were (225nm, 520nm), (225nm, 480nm), (215nm,480nm), and (215nm, 520nm). The group index and effective index were recorded for each corner point.

4.1 Washington Nanofabrication Facility (WNF) silicon photonics process:

The devices were fabricated using 100 keV Electron Beam Lithography [[1]]. The fabrication used silicon-on-insulator wafer with 220 nm thick silicon on 3 μm thick

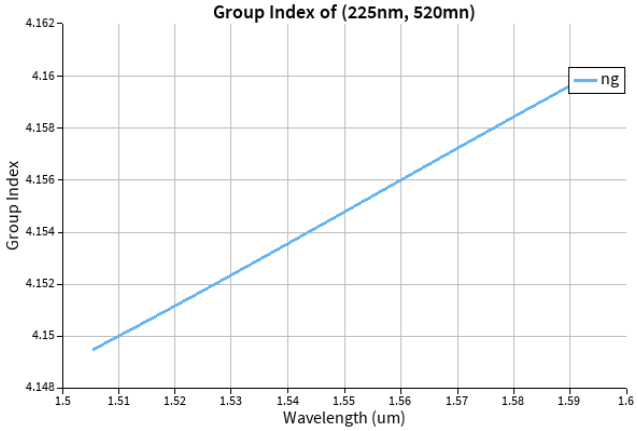

Fig. 6 Group Index for (225nm,520nm)

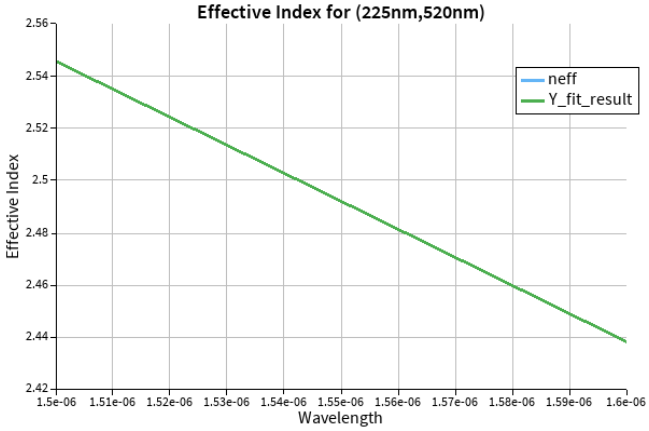

Fig. 7 Effective Index for (225nm,520nm)

silicon dioxide. The substrates were 25 mm squares diced from 150 mm wafers. After a solvent rinse and hot-plate dehydration bake, hydrogen silsesquioxane resist (HSQ, Dow-Corning XP-1541-006) was spin-coated at 4000 rpm, then hotplate baked at 80 °C for 4 minutes. Electron beam lithography was performed using a JEOL JBX-6300FS system operated at 100 keV energy, 8 nA beam current, and 500 μm exposure field size. The machine grid used for shape placement was 1 nm, while the beam stepping grid, the spacing between dwell points during the shape writing, was 6 nm. An exposure dose of 2800 μC/cm2 was used. The resist was developed by immersion in 25% tetramethylammonium hydroxide for 4 minutes, followed by a flowing deionized water rinse for 60 s, an isopropanol rinse for 10 s, and then blown dry with nitrogen. The silicon was removed from unexposed areas using inductively coupled plasma etching in an Oxford Plasmalab System 100, with a chlorine gas flow of 20 sccm, pressure of 12 mT, ICP power of 800 W,

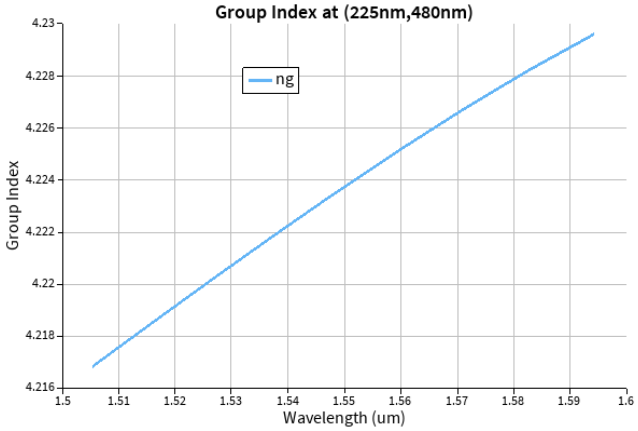

Fig. 8 Group Index at (225nm,480nm)

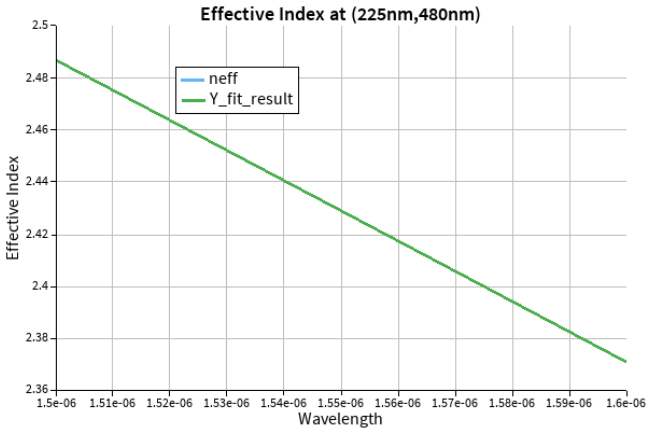

Fig. 9 Effective Index at (225nm,480nm)

bias power of 40 W, and a platen temperature of 20 °C, resulting in a bias voltage of 185 V. During etching, chips were mounted on a 100 mm silicon carrier wafer using perfluoropolyether vacuum oil.

5 Measurement Description

To characterize the devices, a custom-built automated test setup [[2]] with automated control software written in Python was used (`http://siepic.ubc.ca/probestation`). An Agilent 81600B tunable laser was used as the input source and Agilent 81635A optical power sensors as the output detectors. The wavelength was swept from 1500 to 1600 nm in 10 pm steps. A polarization maintaining (PM) fibre was used to maintain the polarization state of the light, to couple the TE polarization into the grating couplers [[3]]. A 90^{o} rotation was used to inject light

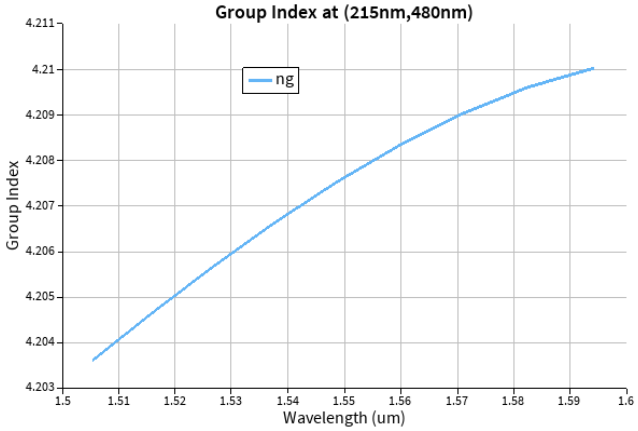

Fig. 10 Group Index at (215nm,480nm)

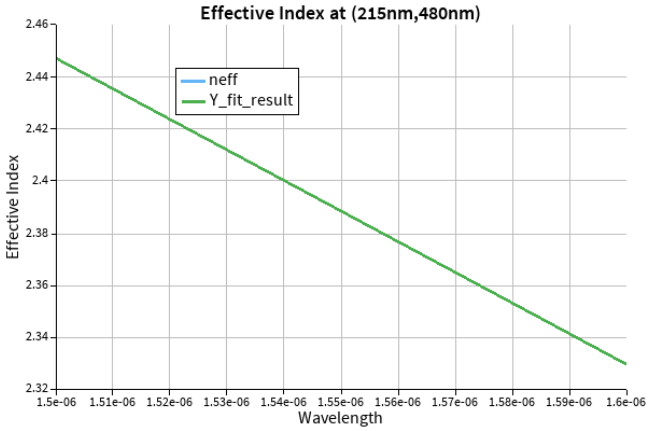

Fig. 11 Effective Index at (215nm,480nm)

into the TM grating couplers [4]. A polarization maintaining fibre array was used to couple light in/out of the chip [www.plcconnections.com].

6 Measurement Results and Analysis

To evaluate the performance of the devices designed, waveguide parameters were extracted from the measurement results, namely the FSR and the group index. To extract these values, an autocorrelation script was modified from course resources and used. The measurement results contained data for wavelengths from 1500 nm to 1580 nm, but to exclude high loss regions, only data corresponding to wavelengths 1530nm to 1580nm was evaluated. Prior to autocorrelation, a calibrated transmission spectrum is created through baseline corrected to allow for

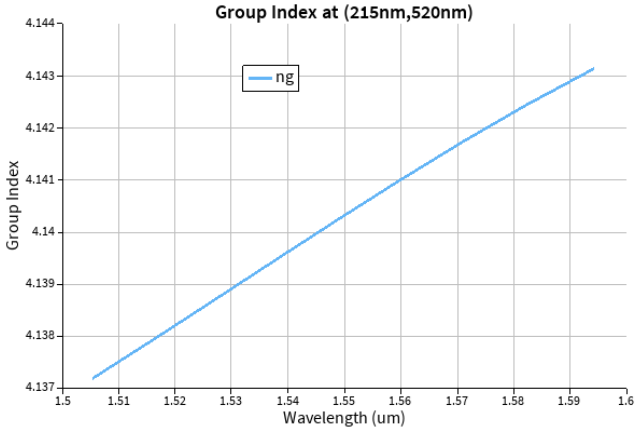

Fig. 12 Group Index at (215nm,520nm)

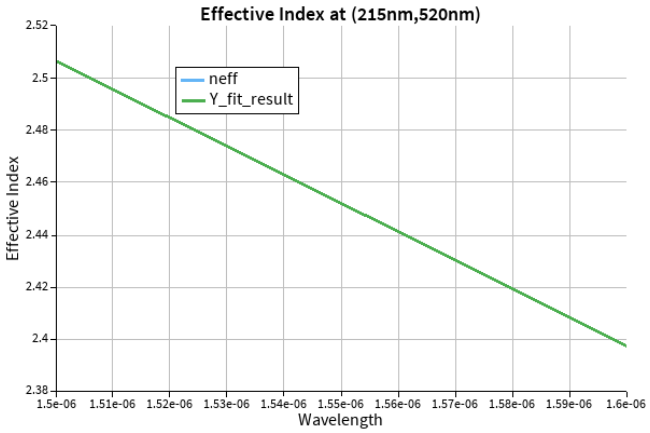

Fig. 13 Effective Index at (215nm,520nm)

better autocorrelation results. Table 2 shows the polynomial order for the baseline correction for each MZI.

Following autocorrelation, results were aggregated into Table 3. Since each path length difference was fabricated and tested twice, there are two measured FSRs and group indexes per path length difference. There is very good agreement between simulated and measured FSRs, and they do not vary depending on the path length difference. However, the measured FSR is always slightly greater than the simulated FSR. There is also very good agreement between simulated and measured group indexes. However, as the length difference increases, the simulated and measured group indexes increases. The results of the measured parameters fit within the corner analysis performed earlier. Additionally, the measured parameters between MZIs with identical path length differences also match quite closely. Below are the graphs for the group index of each MZI.

MZI	Polynomial Fit
1	4
2	2
3	2
4	2
5	2
6	4
7	2
8	2
9	2
10	2

Table 2 MZI vs Polynomial Order

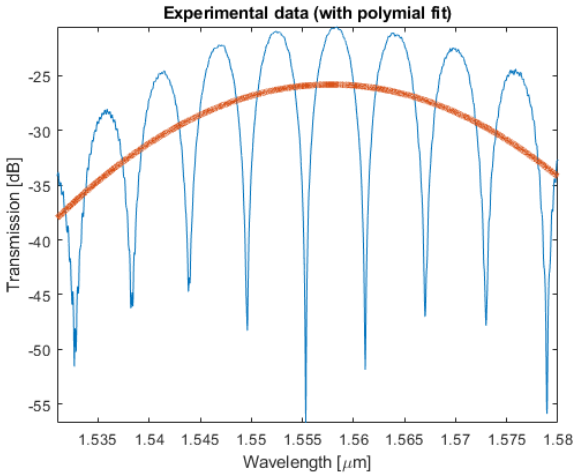

Fig. 14 Uncorrected Spectra for MZI with 100 micron Path Difference

MZI	Path Length Difference(micron)	Simulated FSR(nm)	Simulated Group Index	Measured FSR(nm)	Measured Group Index
1	50	11.44	4.2	11.47	4.2
2	100	5.72	4.2	5.81	4.19
3	150	3.81	4.2	3.85	4.2
4	200	2.86	4.2	2.9	4.19
5	250	2.29	4.2	2.33	4.19
6	50	11.44	4.2	11.46	4.2
7	100	5.72	4.2	5.81	4.19
8	150	3.81	4.2	3.86	4.19
9	200	2.86	4.2	2.89	4.19
10	250	2.29	4.2	2.33	4.19

Table 3 Simulated vs Measured FSR & Group Index

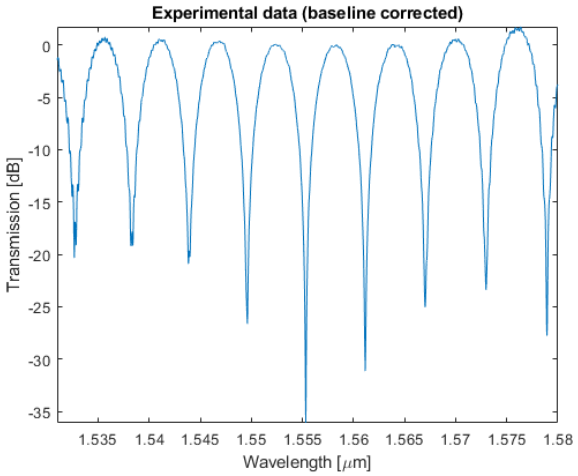

Fig. 15 Baseline Corrected Spectra for MZI with 100 micron Path Difference

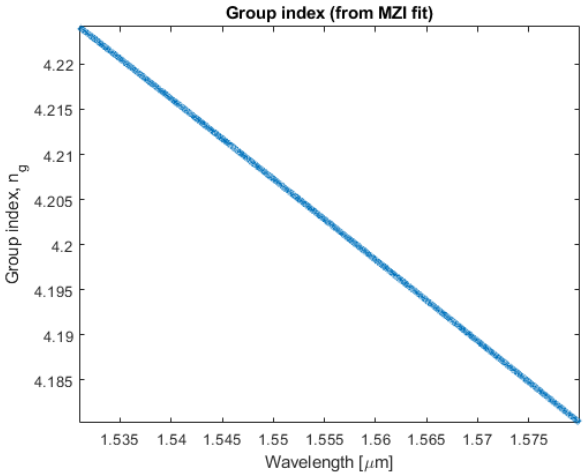

Fig. 16 Group Index for MZI 1

7 Acknowledgements

I/We acknowledge the edX UBCx Phot1x Silicon Photonics Design, Fabrication and Data Analysis course, which is supported by the Natural Sciences and Engineering Research Council of Canada (NSERC) Silicon Electronic-Photonic Integrated Circuits (SiEPIC) Program. The devices were fabricated by Richard Bojko at the University of Washington Washington Nanofabrication Facility, part of the National Science Foundation's National Nanotechnology Infrastructure Network (NNIN), and Cameron Horvath at Applied Nanotools, Inc. Enxiao Luan performed the measurements at The University of British Columbia. We acknowledge Lumer-

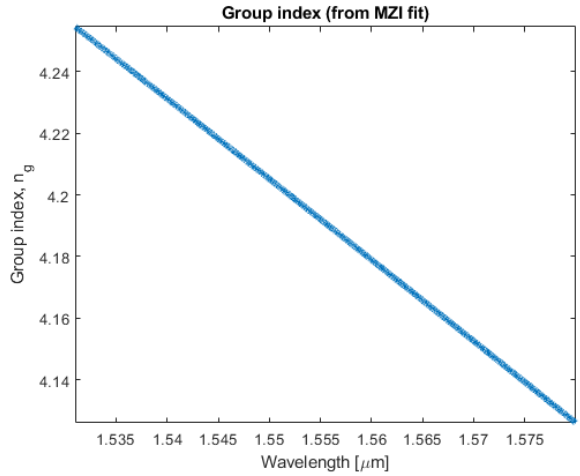

Fig. 17 Group Index for MZI 2

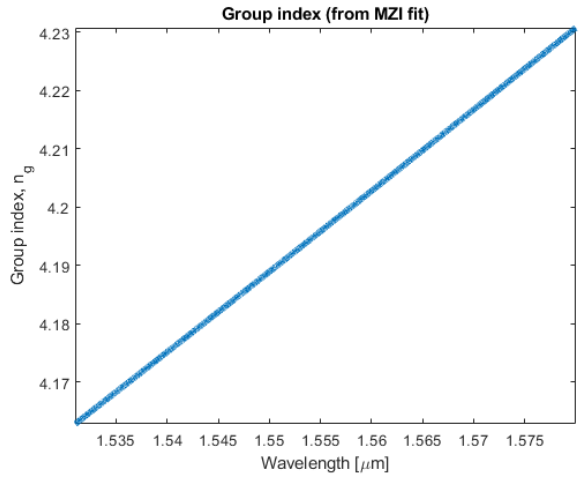

Fig. 18 Group Index for MZI 3

ical Solutions, Inc., Mathworks, Mentor Graphics, Python, and KLayout for the design software.

References

1. Bojko, R.J., Li, J., He, L., Baehr-Jones, T., Hochberg, M., Aida, Y.: Electron beam lithography writing strategies for low loss high confinement silicon optical waveguides. Journal of Vacuum Science & Technology B: Microelectronics and Nanometer Structures **29**(6), 06F309 (2011). DOI 10.1116/1.3653266. URL `http://dx.doi.org/10.1116/1.3653266`

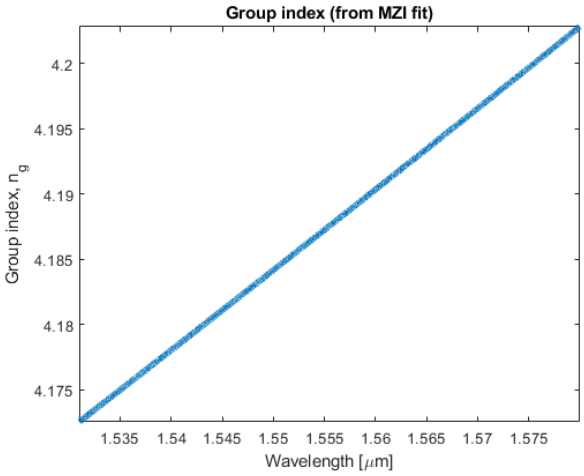

Fig. 19 Group Index for MZI 4

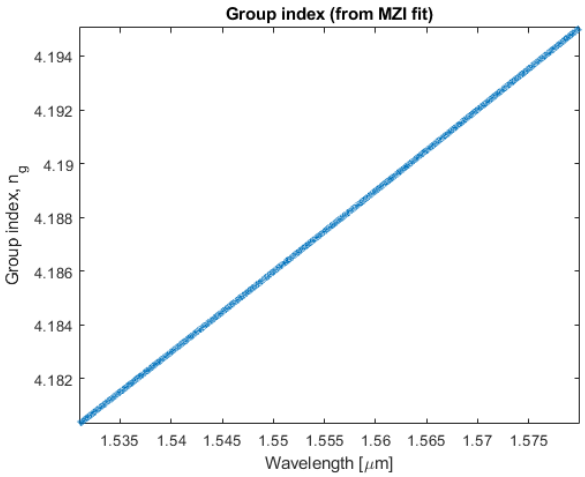

Fig. 20 Group Index for MZI 5

2. Chrostowski, L., Hochberg, M.: Testing and packaging. In: Silicon Photonics Design, pp. 381–405. Cambridge University Press (CUP). DOI 10.1017/cbo9781316084168.013. URL `http://dx.doi.org/10.1017/cbo9781316084168.013`
3. Wang, Y., Wang, X., Flueckiger, J., Yun, H., Shi, W., Bojko, R., Jaeger, N.A.F., Chrostowski, L.: Focusing sub-wavelength grating couplers with low back reflections for rapid prototyping of silicon photonic circuits. Opt. Express **22**(17), 20,652 (2014). DOI 10.1364/oe.22.020652. URL `http://dx.doi.org/10.1364/oe.22.020652`

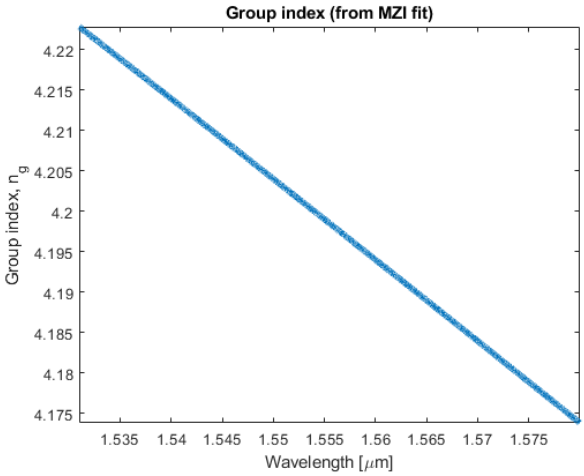

Fig. 21 Group Index for MZI 6

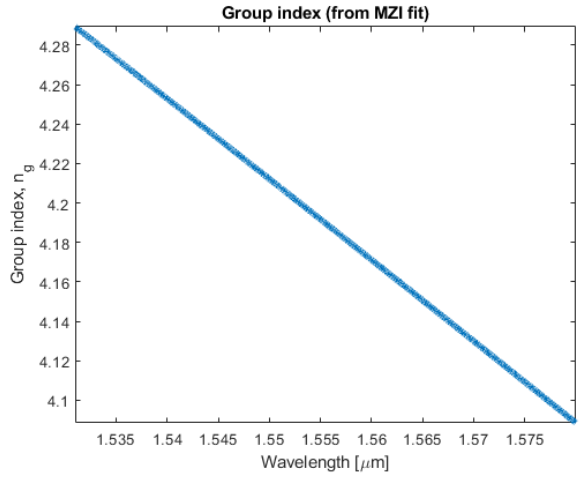

Fig. 22 Group Index for MZI 7

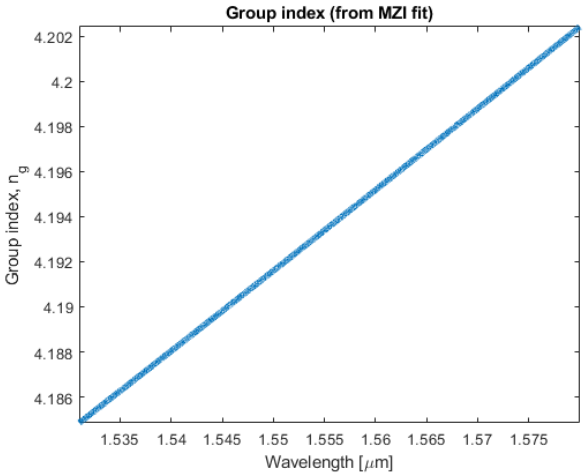

Fig. 23 Group Index for MZI 8

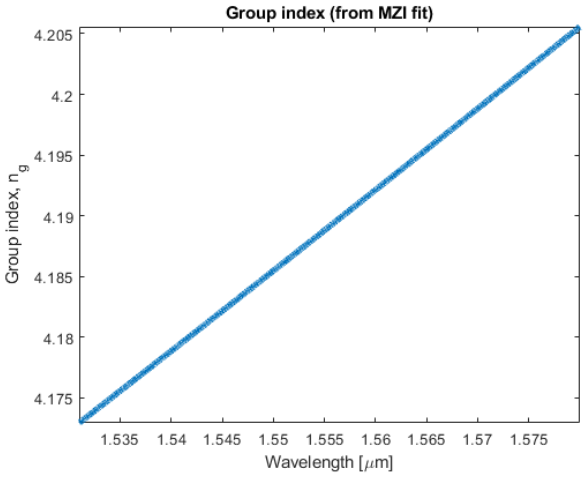

Fig. 24 Group Index for MZI 9

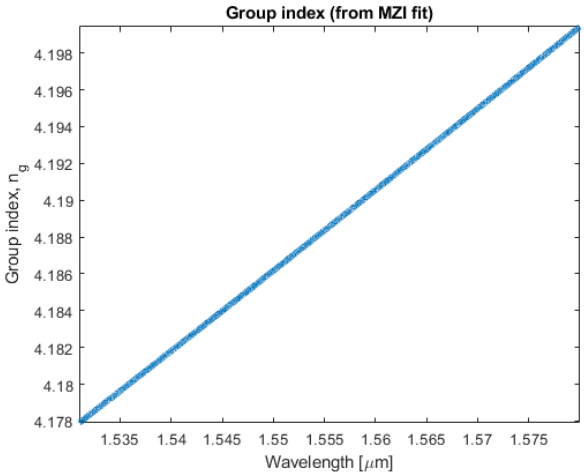

Fig. 25 Group Index for MZI 10